

REPORT

 OPEN ACCESS

The application of mathematical modelling to the design of bispecific monoclonal antibodies

Tamara J. van Steeg^a, Kirsten Riber Bergmann^a, Nazzareno Dimasi^b, Kris F. Sachsenmeier^c, and Balaji Agoram^d

^aLAP&P, Leiden, the Netherlands; ^bAntibody Discovery and Protein Engineering, Medimmune, LLC, Gaithersburg, MD, USA; ^cOncology Research, MedImmune, LLC, Gaithersburg, MD, USA; ^dClinical Pharmacology/DMPK, MedImmune, LLC, Mountain View, CA, USA

ABSTRACT

Targeting multiple receptors with bispecific antibodies is a novel approach that may prevent the development of resistance to cancer treatments. Despite the initial promise, full clinical benefit of this technology has yet to be realized. We hypothesized that in order to optimally exploit bispecific antibody technology, thorough fundamental knowledge of their pharmacological properties compared to that of single agent combinations was needed. Therefore, we developed a mathematical model for the binding of bispecific antibodies to their targets that accounts for the spatial distribution of the binding receptors and the kinetics of binding, and is scalable for increasing valency. The model provided an adequate description of internal and literature-reported *in vitro* data on bispecific binding. Simulations of *in vitro* binding with the model indicated that bispecific antibodies are not always superior in their binding potency to combination of antibodies, and the affinity of bispecific arms must be optimized for maximum binding potency. Our results suggest that this tool can be used for the design and development of the next generation of anti-cancer bispecific compounds.

ARTICLE HISTORY

Received 10 July 2015
Revised 22 December 2015
Accepted 7 January 2016

KEYWORDS

Affinity; avidity;
mathematical; binding;
model; Monovalent;
bispecific; spatial; limitation

Introduction

Targeted anti-cancer approaches often lead to development of resistance and a decrease in patient response.¹ The use of combinations of targeted therapeutics may be a way to avoid resistance and lead to greater efficacy.² In this context, greater efficacy could arise from one or both of 2 mechanisms. First, a combination of agents might affect a greater overall fraction of tumor cells within a heterogeneous population. Alternatively, concomitant targeting of 2 or more pathways known to mediate reciprocal tumor “escape” pathways could prevent net survival of tumor through either pathway.


Affecting two targets in the same treatment regimen can be achieved by combination treatment of (monospecific) monoclonal antibodies (mAbs) or by engineering bispecific antibodies (BSAbs), which are expected to have an advantage over combination antibodies in targeting multiple pathways because of what is termed the “avidity hypothesis.” Specifically, this hypothesis predicts that increased avidity arising from binding of 2 receptors on a target cell leads to greater efficacy than combination therapy with 2 antibody molecules, each binding only a single target receptor.³ This hypothesis has been actively pursued by antibody engineers; for example, molecules targeting both insulin-like growth factor 1 receptor (IGF1R) and the epidermal growth factor receptor (EGFR) have been reported, including tetra-valent BSAbs and an antibody-mimetic construct (avimer).^{4,5} Whereas a number of EGFR-IGF1R targeting bispecific agents have been described, with many showing higher *in vitro* and *in vivo* efficacy than either combination of antibodies

or individual antibodies, none has demonstrated a dramatic improvement in efficacy in clinical trials when compared to combination treatment directed at the same set of targets.^{4–8} The reasons for the lack of this translation from a hypothesis to clinical benefit is unclear, but could possibly be related to limitations in the design of the BSAbs, choice of the target patient population, and/or dose of antibody administered to patients.

We hypothesized that a mathematical analysis of the BSAbs-receptor system in a tumor-like setting may shed light on this discrepancy. Over the years, a number of mathematical models have been suggested to explore the multivalent binding of antibodies to their target receptors.^{9–13} Kaufmann calculated the equilibrium constants for a bivalent molecule (e.g. a mAb) while taking into account spatial limitations in binding.⁹ Spatial limitations dictate that simultaneous attachment of both arms of a BSAbs will only occur if a second receptor is in the vicinity of the first receptor. Müller published a dynamic model for bivalent binding according to the same principles.¹⁰ An important feature of this model is the probability of bivalent binding, which is calculated based on receptor density of a single receptor type and the distance between the 2 arms of the mAb.

More recently, mathematical models that capture heterogeneous bivalent binding, thus binding to 2 different receptor types, were published by Doldán-Martinelli et al and Harms et al.^{11,12,14} In the model proposed by Harms,¹² binding to the cell surface is affected by the concentrations of BSAbs and its receptors, the binding constants and an avidity factor, but the model does not take into account spatial limitations. The model

CONTACT Tamara J. van Steeg  t.vansteeg@lapp.nl

 Supplemental data for this article can be accessed on the publisher's website.

Published with license by Taylor & Francis LLC, © Tamara J. van Steeg, Kirsten Riber Bergmann, Nazzareno Dimasi, Kris F. Sachsenmeier and Balaji Agoram
This is an Open Access article distributed under the terms of the Creative Commons Attribution-Non-Commercial License (<http://creativecommons.org/licenses/by-nc/3.0/>), which permits unrestricted non-commercial use, distribution, and reproduction in any medium, provided the original work is properly cited. The moral rights of the named author(s) have been asserted.

described by Doldán-Martínelli¹¹ does take into account the restriction in binding due to the limited availability of a second binding receptor; however, it does not include the influence of receptors on non-tumor cells. As such, none of the models mentioned above can describe multivalent binding of a BSAb to 2 different receptors with different expression densities on tumor cell surface while accounting for presence of other non-tumor – “decoy” – cells with different receptor expression densities. Our model is the first to capture all of these processes in a single mathematical binding model for BSABs.

Here, we describe the development of a mathematical model for binding of BSABs to their targets. The model includes spatial limitation of bivalent binding and allows the exploration of heterogeneous bivalent binding which may be influenced by varying receptor densities at the cell level, the presence of decoy cells, and BSAB affinities. The model was evaluated using in vitro data generated internally and from literature. We used the model to compare the performance of monovalent BSABs with combination antibodies and tried to answer the following questions: 1) is the avidity hypothesis universally true or are there conditions under which bispecifics are only as good as (or even worse than) combination antibodies?; 2) what is the dependence of the overall binding potency on system factors such as receptor density and presence of “decoy cells”?; and 3) how can this understanding be used in designing optimal BSAB for a particular application?

Results

Virtual experiments: definitions and simulation conditions

Upon administration, an antibody will interact with its target receptors on the tumor. Often, receptors of the same type are expressed on cells other than tumor cells themselves. In this context non-tumor cells expressing targets are referred to as “decoy” cells. Thus, an antibody binds in vivo to both target and decoy receptors. For the simulations in this manuscript, we chose the EGFR/IGFR receptor combination. This model reflects the clinical setting where EGFR is often over-expressed within certain tumors (reviewed in Ref. Fifteen), while IGF1R is more widely expressed in non-tumor tissue than EGFR.¹⁵ Virtual experiments were performed in which binding for a monovalent bispecific to tumor cells expressing EGFR and IGFR was assessed in the absence and presence of decoy cells. Combination treatment of EGFR and IGFR mAbs was used as a benchmark for comparison. For the sake of simplicity, it was assumed that maximization of binding to both EGFR and IGFR on tumor cells was beneficial for efficacy of treatment and binding to any receptor on decoy cells did not lead to efficacy. Total target binding was defined as the sum of EGFR and IGF1R binding on tumor.

Model provided adequate description of in-house and literature data

Fig. 1 (A-C) compare model evaluation against in vitro binding data and Fig. 2 is a comparison against literature-reported data. The only adjusted parameter in this evaluation is the “reaction volume,” which was adjusted for each of the 2 cases (see Supplement S3 and the methods section on model validation). Overall, the model adequately

captured the observed binding for the different cell types and the different mAbs and BSABs. Furthermore, the model adequately predicted the experimental total binding data from the Harms et al paper published in 2012 (Fig. 2).¹⁴ Total binding (black solid line) is the sum of bivalent (gray solid line) and monovalent binding (black broken line). A shift from bivalent to monovalent binding is observed at higher IgG concentrations (Fig. 3, $\log M \text{ IgG} > -9$). For high EGFR expression (A431 cells), this shift is observed as a shoulder in the binding data ($\sim \log M \text{ IgG} = -8$). This shift from bivalent binding toward monovalent binding with increasing concentrations is adequately captured by the model for all cell types (Fig. 2). These simulations show that this model can be used to explore properties of a monovalent BSAB.

Model indicates higher binding potency of BSABs over combination therapy (avidity hypothesis) beyond a threshold receptor density

Fig. 3 shows a comparison of the binding potency of BSABs and combination therapy, starting with a concentration of 1 nM each of the IGFR and EGFR components. In this system, the receptor density of EGFR on tumor cells was varied and the IGF1R expression on tumor cells and decoy cells were assumed to be 10-fold lower and 2-fold higher than EGFR expression on these cells, respectively. The conditions were chosen based on relative EGFR/IGFR receptor density observed in BxPC3 cells (personal communication). The simulation shows that total binding on tumor cells at low receptor densities is less for the BSAB compared to combination treatment ($< 10^5$ receptors per cell, panel A), indicating that the advantage of a BSAB is lost under these conditions. Panel B shows reduced binding of the BSAB to the decoy cells compared to the combination treatment at high receptor densities, indicating preferential binding to tumor cells. Interestingly, binding to decoy cells is reduced to zero for the BSAB at high receptor densities ($> 10^5$ pM), indicating complete preferential binding to the tumor cell as a consequence of avidity. The combination treatment, on the other hand, distributes equally between the tumor and decoy cells. Thus, the differentiation between the BSAB and the combination treatment appears to be directly linked to the receptor density on tumor cells.

Binding potency of BSABs is more sensitive to presence of decoy cells than combination antibodies

Fig. 4 shows the influence of the relative abundance of decoy vs tumor cells on tumor cell binding. Target and decoy cells expressed 1×10^6 and 1.5×10^6 IGF1R per cell, respectively. The number of IGF1R and EGFR were assumed to be comparable on the tumor cell but not identical to allow for differentiation ($\text{IGF1R} = 0.9 \times \text{EGFR}$). With an increase in decoy-target cell ratio (ccr) from 1–5, a rightward shift is observed for the concentration-binding curve of the combination treatment (solid vs. dashed lines) indicating less binding to the tumor cell at a given drug concentration. In contrast, the influence of an increase in decoy cells appears

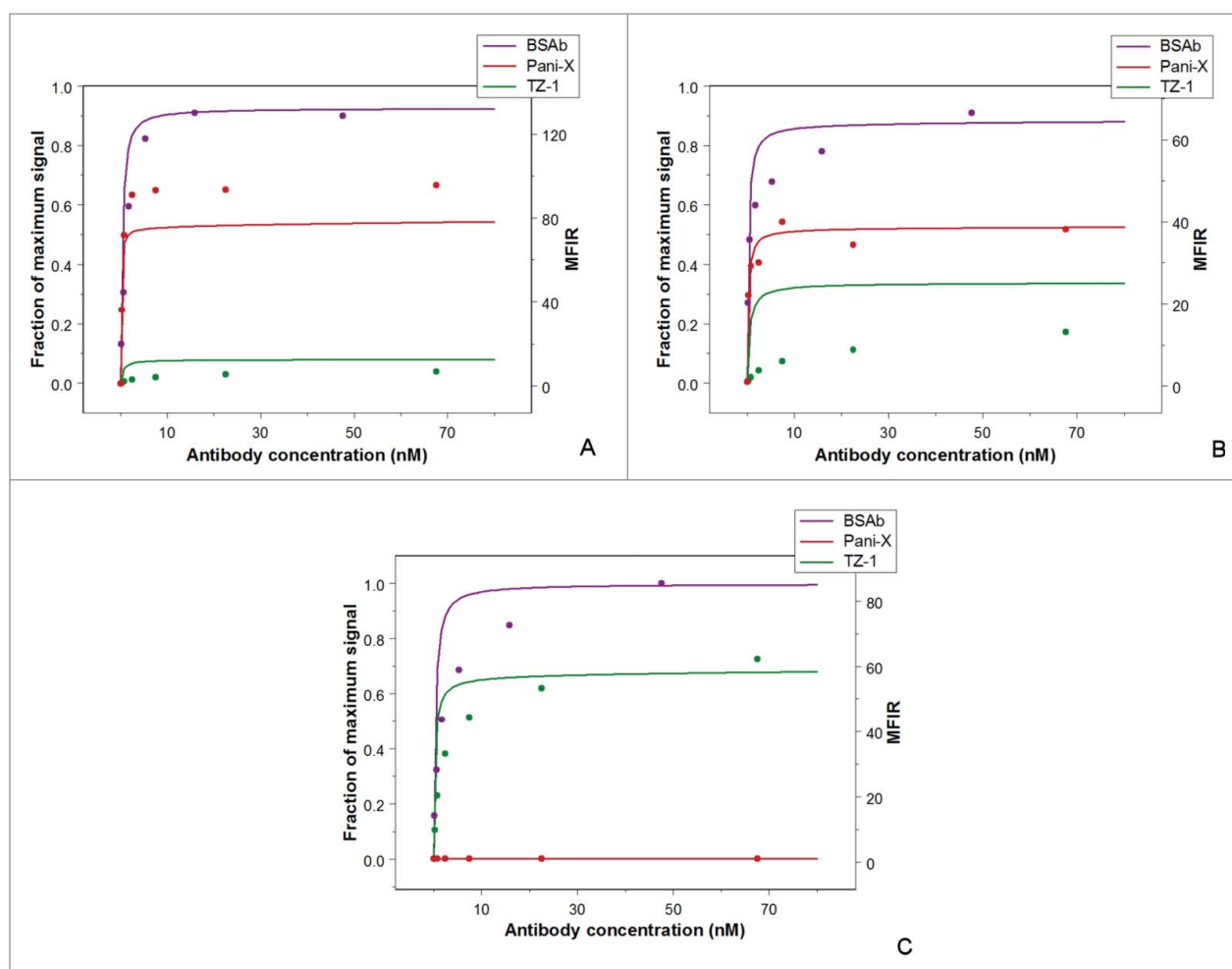


Figure 1. Model verification against binding data of a monovalent BSAb and its reference monoclonal antibodies (anti-EGFR or anti-IGF1R) for different cell types (BxPC-3, H358, NIH3T3). In this simulation, the fraction of the maximal binding signal (left y-axis) was predicted as a function of antibody concentration in nM (x-axis) and plotted against real-life binding data (MFIR, right y-axis). The purple symbols and lines represent the binding data and model prediction for the monovalent BSAb, respectively. The red symbols and lines represent the binding data and model prediction for the anti-EGFR mAb, respectively. The green symbols and lines represent the binding data and model prediction for the anti-IGF1R mAb, respectively. A. Binding to BxPC-3 cells; B. Binding to H358 cells; C. Binding to NIH3T3 (decoy) cells.

to be limited for the BSAb as binding under these conditions as the receptor occupancy is unchanged except at very high levels of BSAb due to the presence of great number of decoy cells.

Binding potency of BSABs is maximized at optimum affinity

We evaluated the influence of receptor affinity on the binding potency of BSABs. Simulations were performed for a high

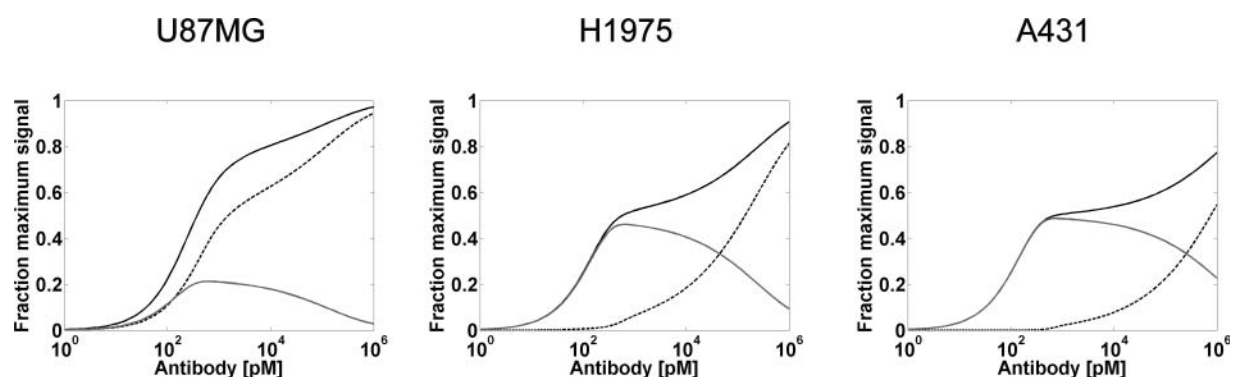


Figure 2. Model verification against binding data from Harms et al. Simulation of total bound (black solid line), bivalent bound (gray solid line) and monovalent bound (black dashed line) plotted as the fraction of the maximum signal (y-axis) against antibody concentration (pM) for a parent antibody using the parameters as reported by Harms et al.¹⁴ A. Simulation for U87MG cells with a receptor density of 5.8×10^4 receptors/cell; B. Simulation for H1975 cells with a receptor density of 3.6×10^5 receptors/cell; C. Simulation for A431 cells with a receptor density of 2×10^6 receptors/cell. The parameters k_{on} and K_D were obtained from the original publication. The reaction volume (V_r) was set to the relevant range reported in the publication (3.4×10^{-5} L). The effective concentration (C_{eff}) was adjusted to 0.01 to reflect the observed binding curve.

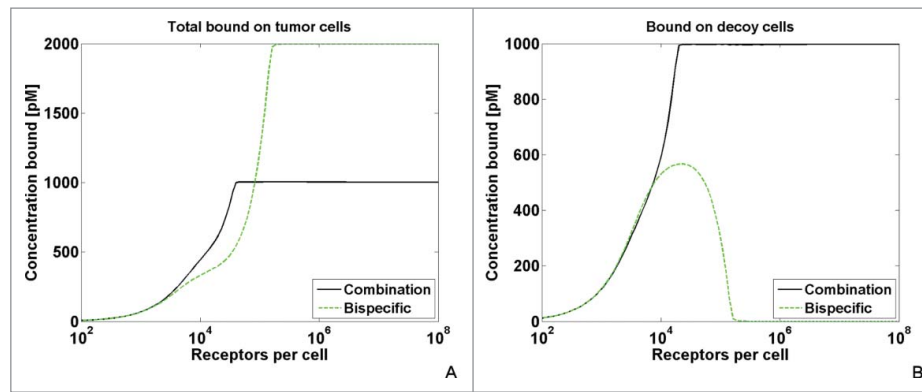


Figure 3. Combination versus Bispecific treatment: Influence of receptor density on target and decoy binding. A. Simulation of total concentration bound at tumor cells in a decoy cell scenario with decoy-target cell ratio of 1; B. Simulation of IGF1R concentration bound at decoy cells (decoy-target cell ratio of 1). Simulations were performed with a fold10- lower receptor density for IGF1R compared to EGFR on tumor cells, which resembles BxPC-3 cells. The receptor density on the decoy cells was assumed to be 2-fold higher than the EGFR receptor density on tumor cells which resembles the difference between tumor cells (BxPC-3) and decoy cells (NIH3T3).

receptor density ($\sim 1 \times 10^6$ receptors/cell) on tumor and decoy cells with decoy-tumor cell ratio of 3. The affinity of BSAb to EGFR was kept constant and that for IGF1R was varied in the range $0.1 - 1 \times 10^6$ pM. Total binding to tumor cells is shown as a function of the antibody concentration (Fig. 5). For a particular concentration of the antibody, an optimum affinity range existed, in this case between $1 \times 10^2 - 1 \times 10^4$ pM, when binding to the tumor cells was maximized. At higher affinity, the BSAb tended to get trapped on decoy cells, thus losing the advantage of the avidity effect (not shown). At very low affinity, avidity had little effect, thereby reducing total and IGF1R binding to tumor cells. It can thus be concluded that an optimum affinity exists that would maximize binding efficiency for a BSAb.

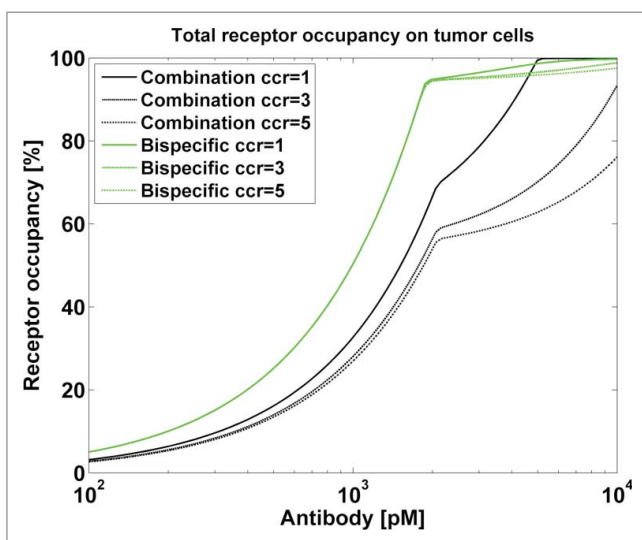


Figure 4. Bispecific vs. Combination treatment: Influence of decoy-tumor cell ratio (ccr). Simulation of total receptor occupancy (y-axis) against antibody concentration (pM). Similar receptor densities for IGF1R and EGFR on tumor cells (EGFR = 1×10^6 receptors/cell, IGF1R = 0.9×10^6 receptors/cell) were assumed, which resembles H-358 cells. The receptor density on the decoy cells was assumed to be 1.5-fold higher than the EGFR receptor density on tumor cells.

Model was applied to design a new anti-EGFR BSAb with improved therapeutic index

Finally, the model was used to design anti-EGFR BSAb targeting different EGFR epitopes that would selectively bind the tumor cells with high EGFR density ($\sim 10^6$ receptors/cell), while avoiding off-target cells such as skin and liver cells, which have lower EGFR density ($\sim 10^3$ receptors/cell), thus providing an improvement over current anti-EGFR therapies. Simulations were performed to predict the binding potency of a BSAb as a function of receptor densities for different BSAb affinities. For the sake of simplicity, the affinity to both epitopes was assumed to be the same and the presence of decoy cells was ignored.

In Fig. 6, the total concentration of receptors bound is plotted against receptor density for BSAb affinities ranging

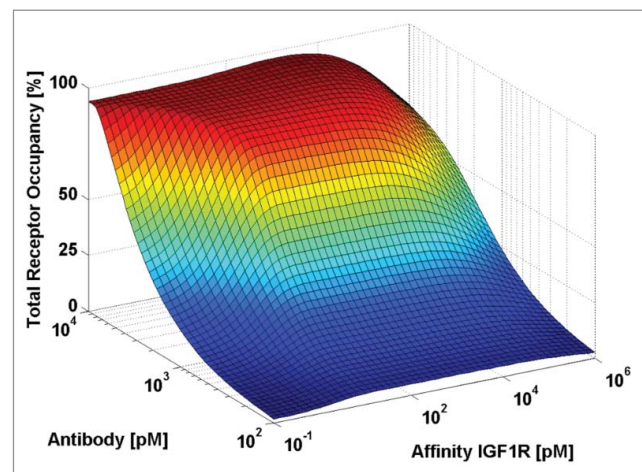


Figure 5. Influence of IGF1R affinity on total binding on tumor cells. A surface plot in which receptor occupancy (%), z-axis) was simulated as function of IGF1R affinity (pM, x-axis) and antibody concentration (pM, y-axis). Simulation of total receptor occupancy on the tumor cell. K_d ranges from high (0.1 pM) to low (1×10^6 pM) affinity for IGF1R. The antibody concentration ranges from 100 to 10000 pM. Simulations were performed for a high receptor density (1×10^6 receptors/cell) on tumor and decoy cells with target-decoy cell ratio of 3. The affinity for EGFR was kept constant to 1 nM (medium affinity).

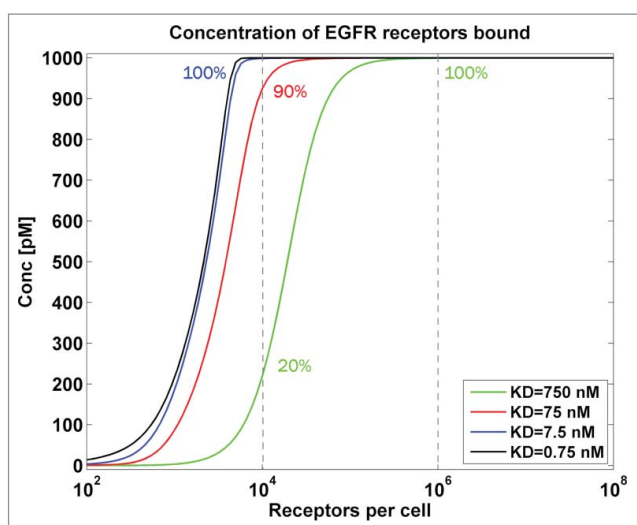


Figure 6. EGFR therapy, total concentration bound for high-high and low-low affinity compounds. Receptor binding as a function of receptor density on the cell surface: the influence of bivalent binding with different affinities. The green, red, blue and black solid lines represent binding of the antibody at an affinity of 750, 75, 7.5 and 0.75 nM, respectively. The black vertical lines indicate the receptor density for decoy cells (low receptor density = 10^4 receptors/cell) and target cells (high receptor density = 10^6 receptors/cell).

from 0.75–750 pM. At high affinity ($K_d \leq 75$ nM), binding to both the low and high density cells is high, whereas at a lower affinity – 750 nM – binding to tumor cells is high, but that to skin and liver cells is minimized (receptor occupancy $\sim 20\%$). This results from the effect of avidity in the “tumor” tissues due to high receptor density and the lack of avidity in “healthy” tissues due to low receptor density.

Discussion

An emerging approach to the treatment of cancer is the use of multi-specific antibodies, which may maximize treatment response, while minimizing side effects.¹⁶ While early investigations have indicated that this approach has promise, the ideal combination of tumor (system) characteristics and antibody (design) parameters to optimize its value are not yet fully understood. We developed a mathematical model of in vitro target binding of BSABs to provide a starting point for

quantitative investigation into this problem. Simulations have provided interesting insights into the design aspects of this class of molecules. We also applied the model in the design of a BSAB with potentially improved tumor-targeting properties compared to a conventional antibody.

In contrast to some previous models,^{12–14} a distinction is made between the rate and the space in which bivalent binding occurs and the distribution of different receptors in the current approach. Furthermore, binding to tumor and decoy cells is distinctly modeled, potentially aiding in understanding the ability of BSABs in maximizing the therapeutic index over mAbs. Once calibrated, verification against available binding data showed the model’s ability to reproduce homogenous bivalent binding (Fig. 2, literature data) and heterogeneous bivalent binding (Fig. 1, in-house experimental data). Despite the large variability in the experimental data, the general trend in the data was adequately captured by the model.

We then used the model to try and understand the complex interactions of a BSAB with its cognate receptors in a tumor-like setting. For the sake of simplicity, we only considered the following aspects of this system: receptor density, decoy-target cell ratio, and antibody affinity under physiologically-relevant conditions. Even under these simplified conditions, simulations using the model highlighted non-intuitive behaviors of the system, which are important for design considerations. For example, Fig. 3 indicates that under conditions of no decoy receptors, for low receptor densities ($<10^4$ receptors per cell), BSAB are less potent than combination treatment. At low receptor densities, the BSAB gets “trapped” on one of its receptors and the other arm is unable to bind due to lack of receptors in the vicinity. Under these conditions, a mAb combination performs better due to lack of steric hindrance. Beyond $\sim 10^5$ receptors/cell, due to the influence of avidity, monovalent binding is greatly minimized (Fig. 3B), whereas the combination therapy does not have this advantage. These receptor density values fall within the relevant ranges observed for in vitro cell systems for oncology (unpublished flow cytometric observations; Table 1), and therefore the simulations have relevance for interpreting in vitro and clinical results.

Off-target binding is generally considered to reduce the therapeutic index, but, compared to combination treatment, this may be less relevant to a BSAB (Fig. 4). In the simulations, the BSAB was shown to be less susceptible to the presence of a large

Table 1. Overview of parameters and origin.

Drug/System	Parameter	Value	Origin
Cell radius	rc (cm)	7.5×10^{-4}	Kaufmann et al., 1992 ⁹
Access radius	r (cm)	4.9×10^{-6}	Calculation based on antibody length ^A
Reaction volume	Vr (L)	7.9×10^{-10}	Obtained by calibration
On rate binding	k_{on} (1/pM/s)	2.2×10^{-6}	Krippendorf et al., 2012, Patel et al., 2010 ^{8,27,28}
		EGFR	IGF1R
Pani-X affinity	K_D (pM)	261	—
TZ-1 affinity	K_D (pM)	—	540
BSAB affinity	K_D (pM)	253	297
BxPC-3 cells	Rcell (receptors/cell)	186013.6	17679.0
H358 cells	Rcell (receptors/cell)	38260.5	23106.5
NIH3T3 cells	Rcell (receptors/cell)	231.3	106317.8

^AActual access radius was calculated to be 49 Å (4.9×10^{-7} cm) based on the length antibody being 70 Å. To account for flexibility and cross linking capacity, in the simulations an apparent access radius of 4.9×10^{-6} cm was used [Ref Kaufmann and Muller].

number of decoy cells than combination treatment. Consequently, the model can be used to design molecules that minimize side-effects.^{17–23}

These two model results suggest that BSABs may show increased tumor binding and efficacy compared to combination treatment, when treating tumors with higher concentrations of the non-decoy target and high decoy to tumor cell ratios. One could speculate that differences between combination treatment and bispecifics are unlikely to be observed if the patient population for which combination treatment works is selected. Choosing the ‘right’ patient population is essential in order to show the benefit of bispecific molecules and this may be one of the reasons for the lack of higher efficacy observed in clinical trials of BSABs compared to mAbs.

Apart from identifying the system (tumor) properties optimal for BSAB treatment, the model also identifies optimal antibody properties to maximize therapy. For example, the model indicates that higher affinity may not necessarily be suitable for preferential tumor targeting, and a lower affinity may provide a higher therapeutic index (Fig. 5 and 6). Both these simulations illustrate the existence of an optimum affinity that is neither too high nor too low. In Fig. 5, high affinity to the decoy receptor results in the BSAB being trapped in decoy cells – very low affinity to the decoy receptor results in lack of avidity and the antibody essentially functions as a monospecific antibody. The optimal affinity spans a wide range (>100 -fold) indicating that maturation of affinity to decoy receptor may not need to be resource-intensive. In Fig. 6, very high affinity results in the loss of specificity to the tumor. To our knowledge, this simulation is the first instance where it has been mathematically shown that the hypothesis of higher selectivity toward high receptor expressing cells is possible. Verification of these predictions are available from studies with early pre-clinical anti-EGFR BSABs that suggest that the use of multi-epitopic binding antibodies might lead to preferential targeting to EGFR-overexpressing tumors rather than normal skin.²⁵

Our simulation studies enable selective use of multi-specific antibodies through an in-depth examination of how and when target density and affinity yield improved target binding. Without such an analysis it is possible that a “more is better” approach may be assumed in the relationship between a therapeutic antibody and its target(s). For example, the simple expression of both antibody targets within a given tumor, regardless of their densities, could lead to a naïve selection of indications or prospective patients, with no regard to how overexpression of one target could actually yield predominantly single-target binding. Assessment of target expression density as described in this study will allow the rational and more precise identification of the patients who are likely to benefit from a particular multi-specific agent, and help design antibodies for specific patient populations. These conclusions can be extended to the field of multi-targeted antibody drug conjugates also.²⁴

One limitation of the model is that it currently only relates the system and design parameters to overall binding potency against the different targets. How this binding

translates to cell killing efficacy is as yet unknown. Also, for the sake of simplicity, the model assumes that the target expression levels do not vary between tumor cells in patients. It is known that this is not always true in patients, even within a single tumor, and as such this may affect the efficacy of a BSAB compared to combination treatment.²⁶ It is important to note that the current analysis of the model is non-exhaustive. For a more comprehensive analysis of in vivo tumor efficacy, other system factors (e.g., variability in receptor expression across tumor/decoy cells, receptor recycling, pharmacokinetics of the BSAB) all need to be taken into account. This model provides a convenient starting point for these explorations.

In conclusion, we developed a new model to describe the binding of BSABs to their target that accounts for the spatial distribution of the binding receptors and the kinetics of binding, and is scalable for increasing valency. The model provided adequate description of internal and literature-reported data on bispecific binding. Model predictions provided interesting, previously unreported, properties of bispecific binding systems, suggesting that this tool can be invaluable in the design and development of the next generation of anti-cancer medicines.

Materials and methods

Computation

Development of the model and simulations were performed using MATLAB software (version 7.11.0, release 2010b, MathWorks, Natick, MA, USA). The model code in MATLAB is provided in S1.

Model for bivalent binding of monovalent BSABs to cell surface receptors

The model for bivalent binding of monovalent BSABs to cell surface receptors is an extension of the model for binding of mAbs published by Müller *et al.*¹⁰ Bivalent binding of antibodies to soluble receptors is dependent on antibody concentration, receptor concentration and binding parameters. For surface-bound receptors, the average distance between receptors may be too large for all receptors to be bound bivalently. Consequently, spatial limitation of binding was implemented in the model. A BSAB is an antibody with 2 arms that bind 2 different receptors. The affinities for the targets and the abundance of both receptor types were considered relevant for bivalent binding. The developed model consists of 2 parts: 1. probability of bivalent binding and 2. kinetics of bivalent binding.

Probability of bivalent binding

The model included the probability of having only one receptor type per sphere. The probability of binding was obtained by dividing the cell surface into areas swept out by the antibody (spheres). The probability of bivalent binding equation are shown in the supplementary materials (S2). It was assumed that: 1) bivalent binding requires 2 receptors in a sphere; 2) probability of binding is dependent on the amount of receptors

in the sphere; 3) receptors on the cell surface are Poisson distributed; and 4) the concentration of receptors accessible depends on receptor density on cell surface and the access radius.

Kinetics of bivalent binding

At low receptor density, not all receptors will have a second receptor in the vicinity to facilitate bivalent binding. Five types of reactions exist for a BSAb: monovalent binding to either EGFR or IGF1R only, monovalent binding to either EGFR or IGF1R with the possibility of a second binding step and bivalent binding to both. Six ordinary differential equations were used to reflect this and are provided in the supplementary materials (S3). A model for the combination of parental antibodies (combination treatment) was implemented according to the same principles. As such, 3 reactions per mAb were used: monovalent binding (with or without possible second binding step) and bivalent binding.

Parameter values

Simulations were performed from a starting concentration of the antibody until steady state binding was reached unless reported otherwise. The starting concentrations of antibody were in the range of those used in the actual experiments with BSABs.

Meaningful simulations were performed using parameter values that were considered to be relevant for the system under investigation. Parameter values were obtained from literature, from physiological concepts or from experiments (Table 1).

The two parental mAbs (TZ-1 and Pani-X) used to construct the BSAb, each with 2 identical binding arms, either anti-EGFR or anti-IGF1R, were used as a reference in the binding experiments.

Experiments were performed to determine the number of receptors on target and decoy cells.

Cell lines were chosen to represent cancer indications of relevance to EGFR and IGF1R clinical approvals and trials. For example, the NCI-H358 non-small cell lung carcinoma cell line is known to harbor a mutation in the Kras oncogene, as well as a deletion in the p53 tumor suppressor gene. Both of these genes are known to be important in human disease. Similarly, the BxPC3 pancreatic adenocarcinoma cell line has been used to study at least one other EGFR-IGF1R BSAb.⁴ The murine NIH 3T3 mouse cell line was engineered to over-express human IGF1R and was chosen as an appropriate “decoy” cell line because it expresses no human EGFR. The relative receptor densities between actual tumor tissues and that of model tumor cell lines are difficult to compare given that tumors require enzymatic dissociation, which can influence conclusions about actual *in situ* receptor density. However, cultured xenograft cell lines were routinely used pre-clinically to model both anti-EGFR (e.g., panitumumab, cetuximab) as well as anti-IGF1R antibodies. Likewise, the decoy-target cell ratio of 1:1 reported here was chosen for simplicity. The cytotoxicity data shown at this ratio was consistent with model predictions when tested at other ratios.

The following parameters were derived: 1) The dissociation rate (k_{off} , k_{offy}) was calculated ($K_D = k_{off} / k_{on}$); 2) the volume of the sphere (V_s) was calculated based on the access radius; 3) the cell surface was obtained from the cell radius (rc); and 4) the receptor density calculated using the cell surface and the number of receptors per cell.

Model qualification

The model validity was assessed prior to the simulations. Firstly, the model was verified against in-house binding data generated for an anti-EGFR mAb, an anti-IGF1R mAb and a BSAb targeting both. The cell lines expressed varying levels for EGFR and IGF1R. For BxPC-3 cells, a high and medium expression level was observed for EGFR and IGF1R, respectively (Table 1). Adequate prediction of the observed binding curves was obtained by adjusting the reaction volume only (Table 1, Fig. 1).

Harms *et al.* published data obtained from flow cytometry experiments for bivalent binding of IgG and reported monovalent binding parameters, obtained using KinExA.¹⁴ The data and parameters available provided an excellent opportunity to verify the model for bivalent binding of parental arm antibodies. Our model adequately predicted the data for IgG binding to cell lines representing low, medium and high expression levels of EGFR (Fig. 2). The reaction volume ($V_r = 3.4 \times 10^{-5}$ L), the binding parameters (k_{on} , k_{off} , K_D) and the receptor density on the different cell types were implemented based on those reported. The effective concentration was modified to resemble the more pronounced monovalent binding at higher drug concentrations ($C_{eff} = 0.01$).

Disclosure of potential conflicts of interest

ND, BA and KS acknowledge that they are employees of Medimmune, LLC, TS and KB were paid consultants.

Acknowledgments

The authors acknowledge Qihui Huang for performing the experiments. In addition, we thank the Medimmune Antibody Discovery and Protein Engineering team for their work on TZ-1.

References

1. Groenendijk FH, Bernards R. Drug resistance to targeted therapies: Déjà vu all over again. *Mol Oncol* 2014; 12:1-17; PMID:24910388; <http://dx.doi.org/10.1016/j.molonc.2014.05.004>.
2. Holohan C, Van Schaeybroeck S, Longley DB, Johnston PG. Cancer drug resistance: an evolving paradigm. *Nat Rev Cancer* 2013; 13:714-26; PMID:24060863; <http://dx.doi.org/10.1038/nrc3599>.
3. Mazor Y, Oganessian V, Yang C, Hansen A, Wang J, Liu H, Sachsenmeier K, Carlson M, Gadre D V, Borrok MJ, et al. Improving target cell specificity using a novel monovalent bispecific IgG design. *MAbs* 2015; 7:37-41 PMID:25621507; <http://dx.doi.org/10.1080/19420862.2015.1007816>.
4. Croasdale R, Wartha K, Schanzer JM, Kuenkele K-P, Ries C, Mayer K, Gassner C, Wagner M, Dimoudis N, Herter S, et al. Development of tetravalent IgG1 dual targeting IGF-1R-EGFR antibodies with potent tumor inhibition. *Arch Biochem Biophys* 2012; 526:206-18; PMID:22464987; <http://dx.doi.org/10.1016/j.abb.2012.03.016>

5. Dong J, Sereno A, Aivazian D, Langley E, Miller BR, Snyder WB, Chan E, Cantele M, Morena R, Joseph IBJK, et al. A stable IgG-like bispecific antibody targeting the epidermal growth factor receptor and the type I insulin-like growth factor receptor demonstrates superior anti-tumor activity. *MAbs* 2011; 3:273-88; PMID:21393993; <http://dx.doi.org/10.4161/mabs.3.3.15188>
6. Schanzer JM, Wartha K, Croasdale R, Moser S, Künkele K-P, Ries C, Scheuer W, Duerr H, Pompeiati S, Pollman J, et al. A Novel Glycoengineered Bispecific Antibody Format for Targeted Inhibition of Epidermal Growth Factor Receptor (EGFR) and Insulin-like Growth Factor Receptor Type I (IGF-1R) Demonstrating Unique Molecular Properties. *J Biol Chem* 2014; 289:18693-706; PMID:24841203; <http://dx.doi.org/10.1074/jbc.M113.528109>
7. Emanuel SL, Engle LJ, Chao G, Zhu R-R, Cao C, Lin Z, Yamniuk AP, Hosbach J, Brown J, Fitzpatrick E, et al. A fibronectin scaffold approach to bispecific inhibitors of epidermal growth factor receptor and insulin-like growth factor-I receptor. *MAbs* 2011; 3:38-48; PMID:21099371; <http://dx.doi.org/10.4161/mabs.3.1.14168>
8. Lu D, Zhang H, Koo H, Tonra J, Balderes P, Prewett M, Corcoran E, Mangalampalli V, Bassi R, Anselma D, et al. A fully human recombinant IgG-like bispecific antibody to both the epidermal growth factor receptor and the insulin-like growth factor receptor for enhanced anti-tumor activity. *J Biol Chem* 2005; 280:19665-72; PMID:15757893; <http://dx.doi.org/10.1074/jbc.M500815200>
9. Kaufman EN, Jain RK. Effect of bivalent interaction upon apparent antibody affinity: experimental confirmation of theory using fluorescence photobleaching and implications for antibody binding assays. *Cancer Res* 1992; 52:4157-67; PMID:1638531
10. Müller KM, Arndt KM, Plückthun A. Model and simulation of multivalent binding to fixed ligands. *Anal Biochem* 1998; 261:149-58; PMID:9716417; <http://dx.doi.org/10.1006/abio.1998.2725>
11. Doldán-Martelli V, Guantes R, Míguez DG. A mathematical model for the rational design of chimeric ligands in selective drug therapies. *CPT pharmacometrics Syst Pharmacol* 2013; 2:e26; PMID:23887616; <http://dx.doi.org/10.1038/psp.2013.2>
12. Harms BD, Kearns JD, Iadevaia S, Lugovskoy A. Understanding the role of cross-arm binding efficiency in the activity of monoclonal and multispecific therapeutic antibodies. *Methods* 2014; 65:95-104; PMID:23872324; <http://dx.doi.org/10.1016/j.ymeth.2013.07.017>
13. Chudasama VL, Zutshi A, Singh P, Abraham AK, Mager DE, Harrold JM. Simulations of site-specific target-mediated pharmacokinetic models for guiding the development of bispecific antibodies. *J Pharmacokinet Pharmacodyn* 2015; 42(1):1-18; PMID:25559227; <http://dx.doi.org/10.1007/s10928-014-9401-1>
14. Harms BD, Kearns JD, Su S V, Kohli N, Nielsen UB, Schoeberl B. Optimizing properties of antireceptor antibodies using kinetic computational models and experiments. *Methods Enzymol* 2012; 502:67-87; PMID:22208982; <http://dx.doi.org/10.1016/B978-0-12-416039-2.00004-5>
15. Arteaga C. ErbB-targeted therapeutic approaches in human cancer. *Exp Cell Res* 2003; 284:122-30; PMID:12648471; [http://dx.doi.org/10.1016/S0014-4827\(02\)00104-0](http://dx.doi.org/10.1016/S0014-4827(02)00104-0)
16. Kortt AA, Dolezal O, Power BE, Hudson PJ. Dimeric and trimeric antibodies: high avidity scFvs for cancer targeting. *Biomol Eng* 2001; 18:95-108; PMID:11566601; [http://dx.doi.org/10.1016/S1389-0344\(01\)00090-9](http://dx.doi.org/10.1016/S1389-0344(01)00090-9)
17. Gorovits B, Krinos-Fiorotti C. Proposed mechanism of off-target toxicity for antibody-drug conjugates driven by mannose receptor uptake. *Cancer Immunol Immunother* 2012; 62:217-23; PMID:23223907; <http://dx.doi.org/10.1007/s00262-012-1369-3>
18. Gillespie AM, Broadhead TJ, Chan SY, Owen J, Farnsworth AP, Sopwith M, Coleman RE. Original article Phase I open study of the effects of ascending doses of the cytotoxic. *Ann Oncol* 2000; 11:735-41; PMID:10942064; <http://dx.doi.org/10.1023/A:1008349300781>
19. Giles FJ, Kantarjian HM, Kornblau SM, Thomas DA, Garcia-Manero G, Waddelow TA, David CL, Phan AT, Colburn DE, Rashid A, et al. Mylotarg (gemtuzumab ozogamicin) therapy is associated with hepatic venoocclusive disease in patients who have not received stem cell transplantation. *Cancer* 2001; 92:406-13; PMID:11466696; [http://dx.doi.org/10.1002/1097-0142\(20010715\)92:2%3c406::AID-CNCR1336%3e3.0.CO;2-U](http://dx.doi.org/10.1002/1097-0142(20010715)92:2%3c406::AID-CNCR1336%3e3.0.CO;2-U)
20. Onda M, Willingham M, Wang Q -C, Kreitman RJ, Tsutsumi Y, Nagata S, Pastan I. Inhibition of TNF- Produced by Kupffer Cells Protects Against the Nonspecific Liver Toxicity of Immunotoxin Anti-Tac (Fv)-PE38, LMB-2. *J Immunol* 2000; 165:7150-6; PMID:11120846; <http://dx.doi.org/10.4049/jimmunol.165.12.7150>
21. Onda M, Kreitman RJ, Vasmatzis G, Lee B, Pastan I. Reduction of the nonspecific animal toxicity of anti-Tac(Fv)-PE38 by mutations in the framework regions of the Fv which lower the isoelectric point. *J Immunol* 1999; 163:6072-7; PMID:10570296
22. Batelli MG, Buonamici L, Politio L, Bolognesi A, Stirpe F. Hepatotoxicity of ricin, saporin or a saporin immunotoxin: xanthine oxidase activity in rat liver and blood serum. *Virchows Arch* 1996; 427:529-35; PMID:8624583
23. Mosure KW, Henderson a J, Klunk LJ, Knipe JO. Disposition of conjugate-bound and free doxorubicin in tumor-bearing mice following administration of a BR96-doxorubicin immunoconjugate (BMS 182248). *Cancer Chemother Pharmacol* 1997; 40:251-8; PMID:9219510; <http://dx.doi.org/10.1007/s002800050655>
24. Cao Y, Lam L. Bispecific antibody conjugates in therapeutics. 2003; 55:171-97; PMID:12564976
25. Chittenden TD, Setiady YY, Park PU, Ponte JF, Dong L, Skaletskaya A, Carrigan CN, Villaluz AA, Pinkas J, Lutz RJ, Lambert JM. IMGN289, an EGFR-targeting antibody-maytansinoid conjugate with potent activity against non-small cell lung cancer (NSCLC) regardless of dependency on EGFR pathway. *Cancer Res* 2013; 73:Abstract nr 5467; <http://dx.doi.org/10.1158/1538-7445.AM2013-5467>
26. Burrell RA, Swanton C. Tumour heterogeneity and the evolution of polyclonal drug resistance. *Mol Oncol* 2014; 8(6):1095-111; PMID:25087573; <http://dx.doi.org/10.1016/j.molonc.2014.06.005>
27. Krippendorff B-F, Oyarzún D a, Huisinga W. Predicting the F(ab)-mediated effect of monoclonal antibodies in vivo by combining cell-level kinetic and pharmacokinetic modelling. *J Pharmacokinet Pharmacodyn* 2012; 39:125-39; PMID:22399130; <http://dx.doi.org/10.1007/s10928-012-9243-7>
28. Patel D, Guo X, Ng S, Melchior M, Balderes P, Burtrum D, Persaud K, Luna X, Ludwig DL, Kang X. IgG isotype, glycosylation, and EGFR expression determine the induction of antibody-dependent cellular cytotoxicity in vitro by cetuximab. *Hum Antibodies* 2010; 19:89-99; PMID:21178280; <http://dx.doi.org/10.3233/HAB-2010-0232>